Colloid and Polymer Science (2023) 301:417–431
https://doi.org/10.1007/s00396-023-05075-4

ORIGINAL CONTRIBUTION

Self-assembly in newly synthesized dual-responsive double hydrophilic block copolymers (DHBCs) in aqueous solution

Shotaro Yukioka[1] · Shin-ichi Yusa[1] · Virendra Prajapati[2] · Ketan Kuperkar[2] · Pratap Bahadur[3]

Received: 26 December 2022 / Revised: 31 January 2023 / Accepted: 8 February 2023 / Published online: 2 March 2023

Abstract

Double hydrophilic diblock copolymers (DHBCs) with a zwitterionic block of poly[2-(methacryloyloxyethyl phosphorylcholine)] (PMPC) having degree of polymerization (DP) ($n = 25$) and other as thermo/pH-responsive poly[2-(dimethylaminoethyl methacrylate)] (PDMAEMA) block with DP ($n = 24$ and 48) abbreviated as $PMPC_{25}$-*b*-$PDMAEMA_n$ were synthesized using reversible addition-fragmentation chain transfer (RAFT). The influence of the DP of the PDMAEMA block in both the DHBCs in different environments like pH, temperature, and salt concentration was studied exhaustively using proton nuclear magnetic resonance spectroscopy (^{1}H-NMR) and gel-permeation chromatography (GPC). Additionally, the molecular interaction between the blocks was predicted from the optimized descriptors using a computational simulation framework. The self-assembly leading to successive micellization is examined from scattering techniques in the applied stimuli environment. The micellization was favored in alkaline pH and in the presence of salt, particularly for the DHBC with a high DP.

Keywords Stimuli-responsive block copolymer · Self-assembly · Micelles · Scattering · Computational simulation

Introduction

Block copolymers (BCPs) are macromolecules that have grabbed a keen research interest due to their unique chemical features and displaying very fine solution properties [1]. Also, BCPs with one or both blocks responsive to stimuli (temperature, ionic strength, electromagnetic radiation, electric or magnetic fields, and mechanical stress) are even more interesting as they self-assemble to nano-size core–shell aggregates [2, 3]. Advances in controlled polymerization techniques (CRP) such as reversible addition-fragmentation chain transfer (RAFT), atom-transfer radical polymerization (ATRP), stable free radical polymerization (SFRP), etc. have enabled the synthesis of BCPs with more definite structure and tailor-made molecular characteristics (controlled molecular weight, composition of blocks, and low polydispersity) using a variety of monomers [4]. Amongst these approaches, the advantage of RAFT polymerization has proved to be very versatile for the creation of stimuli-responsive polymers (SRP) [5]. Such SRP systems respond quickly to the changes in their environment by producing dramatic and enhanced physical and chemical changes which enable them to get applied in biosensing, drug delivery, smart coatings, tissue engineering, etc. [6–8].

Recently, considerable attention has been focused on double-hydrophilic block copolymers (DHBCs). They form micelles in response to changes in temperature, pH, or ionic strength [9]. When either of these stimuli is applied, one of the blocks turns into colloidal aggregates to become more stable, while the other block turns insoluble in water. Most

Highlights
- $PMPC_{25}$-*b*-$PDMAEMA_n$ are dual (thermo-and pH-) responsive double hydrophilic block copolymers (DHBCs).
- $PMPC_{25}$-*b*-$PDMAEMA_n$ ($n = 24$ and 48) diblock copolymers were synthesized via RAFT and the correct synthesis was confirmed from spectral study.
- Self-assembly and micellar growth of these DHBCs are examined using scattering methods as a function of the applied stimuli (temperature and pH).
- Molecular interactions in DHBCs are discussed using the evaluated optimized computational descriptors.

✉ Ketan Kuperkar
ketankuperkar@gmail.com

[1] Department of Applied Chemistry, Graduate School of Engineering, University of Hyogo (UH), 2167 Shosha, Himeji 671-2280, Japan

[2] Department of Chemistry, Sardar Vallabhbhai National Institute of Technology (SVNIT) Ichchhanath, Surat 395007, Gujarat, India

[3] Department of Chemistry, Veer Narmad South Gujarat University (VNSGU), Surat 395007, Gujarat, India

thermoresponsive and pH-responsive BCPs are made up of two neutral polymer blocks: one with a lower critical solution temperature (LCST) and another with a neutral or polyelectrolyte block. Due to this type of chemical features, DHBCs have gained increasing scope in the field of biomedical applications [10–12].

Zwitterionic polymeric (poly zwitterion) compounds have laid the groundwork for their enormous potential in antifouling coatings, biosensors and drug delivery because of the strong intramolecular and intermolecular interactions caused by the presence of opposing (positive and negative) charges in its structure [13]. The biocompatible zwitterionic polymer such as poly[2-(methacryloyloxyethyl phosphorylcholine)] (PMPC) has acquired a bright scope for biological applications. It possesses an anionic phosphate group and a cationic quaternary ammonium group. Despite these charged groups, PMPC is not considered a surface-active component [14, 15]. The pendant phosphorylcholine group in PMPC exhibits a polar nature and is water-loving (highly hydrophilic) of phosphatidylcholine that creates a cell membrane, which makes it an excellent biocompatible component [16]. Even studies have reported the unique hydrogel properties with high ionic strength observed for PMPC. Though MPC is biocompatible, the metallic catalyst used in ATRP processes leaves harmful residue on its surface. This drawback limits its usage in biological applications. However, the RAFT approach overcomes this limitation [17].

In addition, the temperature and pH-responsive BCPs have captured considerable interest in bioengineering and biotechnology applications. Poly[2-(dimethylaminoethyl methacrylate)] (PDMAEMA) is a well-known instance of conveniently prepared SRP that significantly changes its behavior in a controlled manner with temperature and pH [18]. Anionic and CRP methods like ATRP and RAFT may readily produce PDMAEMA with regulated molecular weights, well-defined chain ends, and diverse macromolecular (such as homo, block, branch or star, and graft) structure copolymers [19, 20]. Being a weak pH-sensitive polybase due to the protonation of the tertiary amine groups at the end of the amine group, PDMAEMA becomes soluble in water at neutral and in acidic pH media. PDMAEMA has longer hydrophobic groups that favor hydrophobic interactions at high pH and creates the "*hypercoiled*" conformations. Depending on the pH, the tertiary amine groups in its main backbone can be made charged or uncharged. PDMAEMA homopolymer precipitates abruptly above pH 7.5 due to amino group deprotonation, followed by the hydrophobic molecular interactions, making it water-soluble at the temperature below LCST and turns insoluble at elevated temperatures exhibiting thermoresponsive behavior [21, 22]. The tertiary amine groups are protonated and positively charged at low pH levels, which causes PDMAEMA to change into a typical water-soluble weak cationic polyelectrolyte [23, 24].

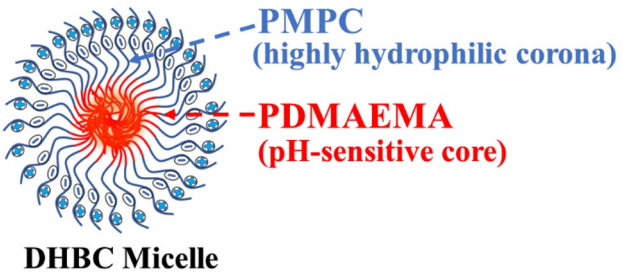

Scheme 1 Conceptual illustration of the micellar constitution in DHBC (PMPC-*b*-PDMAEMA)

Furthermore, the LCST of PDMAEMA in water varies from 35 to 45 °C based on the molecular weight and polymer content, ionic strength, and concentration. The hydrophobicity of PDMAEMA above the LCST promotes the reversible self-assembly of the DHBCs [25]. In the following, depending on the length of the PDMAEMA block, spherical polymeric micelles or ellipsoidal micelles are formed and the ability to produce these variations in morphologies in response to the changes in temperature and/or pH opens up new possibilities for such entities to be developed as multi-responsive nanocarriers especially in the biomedical field [21, 26–28].

Optimizing such copolymeric (PMPC and PDMAEMA) combinations that respond to stimuli is an interesting topic. In recent years, there has been an increase in research focusing on the use of such SRP which exhibits excellent nanoscale core–shell micellar aggregates for varied applications [29–31]. Here, we concentrate on DHBC corona-form having highly hydrophilic diblock copolymers with PMPC-block and the temperature/pH-sensitive PDMAEMA-core-forming block [32–34]. The micelle formed constitutes of the hydrophilic copolymer building block (PMPC) that forms the corona, or outer layer, whereas the hydrophobic building block (PDMAEMA) makes up the inner core (Scheme 1). That enhances the potential for these pH-responsive micelles as nanoscale carriers in drug delivery systems [35, 36].

With this, our study intends to explore the nanoscale self-assembly and aggregation behavior of the synthesized PMPC-*b*-PDMAEMA (DHBCs) in aqueous solution with varying DP of PDMAEMA ($n = 24$ and 48) but constant DP of PMPC block ($n = 25$) via RAFT polymerization. In addition to this, the role of stimuli (pH and temperature) and salt (NaCl) in such DHBCs is also examined using spectral (^{1}H-NMR), and scattering (DLS, and SANS) techniques to infer the details on micellar parameters along with the morphological changes in aqueous solution. Computational simulation approach offers an insight in terms of stable interaction between the well-pronounced polymeric sequences: MPC, DMAEMA, and MPC-*b*-DMAEMA using the molecular orbital energy levels.

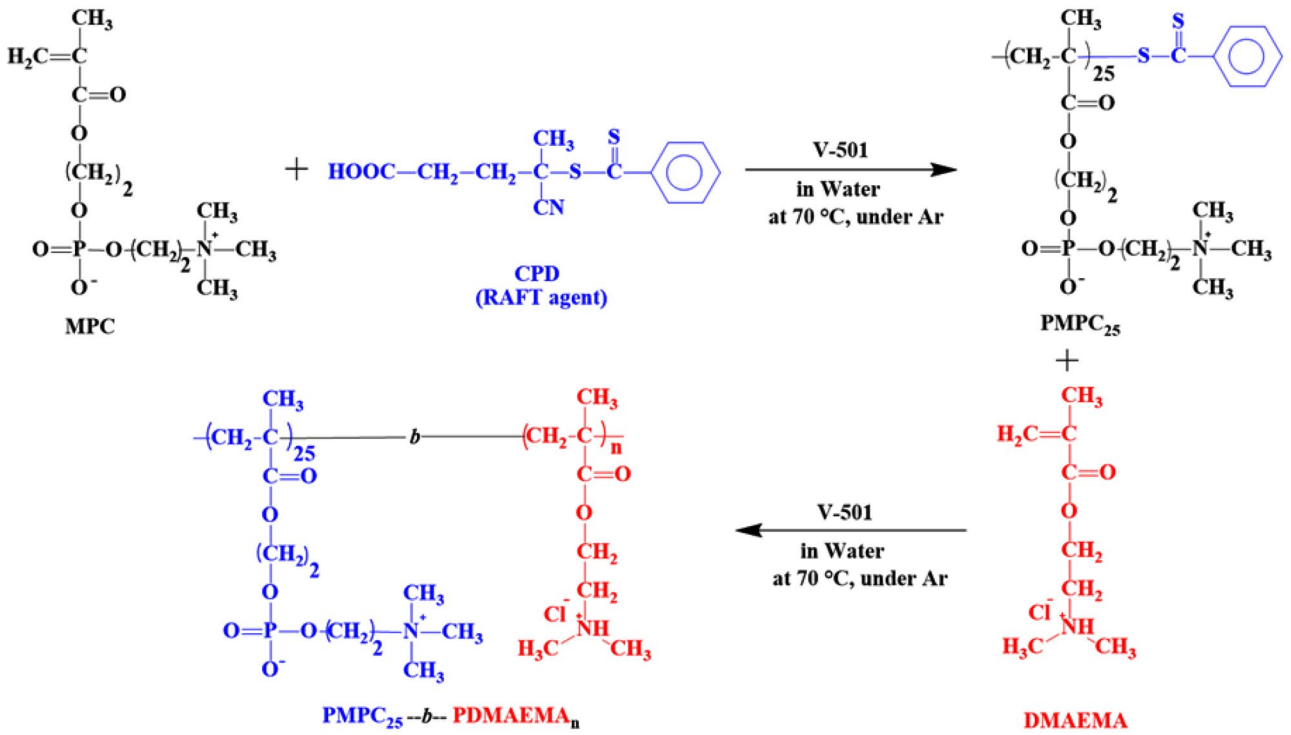

Scheme 2 Synthesis route of $PMPC_{25}$-*b*-$PDMAEMA_n$ (n = 24 and 48)

Experimental section

Materials

For this study, we used 2-(Methacryloyloxy) ethylphosphorylcholine (MPC) supplied by NOF Co. Ltd., Japan; 2-(dimethylamino) ethyl methacrylate (DMAEMA, 99%), and 4,4′-azobis (4-cyanopentanoic acid) (V-501, 98%) from Wako Pure Chemical Industries Ltd., Japan. According to a method described in the literature, 4-cyanopentanoic acid dithiobenzoate (CPD) was produced [19]. Millipore water from Milli-Q system was employed for sample solution preparation. Sodium chloride (NaCl) from Fisher Scientific, India and deuterium oxide (D_2O, 99.9 atom % D) from Sigma-Aldrich, USA were utilized as received.

Methods

Proton nuclear magnetic resonance spectroscopy (^{1}H-NMR)

Bruker DRX-500 spectrometer operating at 500 MHz was used to record ^{1}H-NMR spectra. The synthesized diblock copolymer sample solution was prepared using D_2O as solvent at room temperature. The pH of the sample was varied by adding different amounts of NaOD (deuterated sodium hydroxide) and DCl (deuterium chloride) in D_2O solutions to generate the basic and acidic solution environment respectively. The resulting chemical shifts were then recorded on the δ (ppm) scale [37].

Gel-permeation chromatography (GPC)

GPC measurements for $PMPC_{25}$, $PMPC_{25}$-*b*-$PDMAEMA_n$ (n = 24 and 48) were executed using a refractive index (RI) detector with a Shodex OHpak SB-804 HQ guard column and a UV detector at a temperature of 40 °C. The elution was 0.5 M aqueous acetic acid containing 0.3 M sodium sulfate (Na_2SO_4) with a flow rate = 1.0 mL/min. The M_n and *Mw/Mn* of the examined DHBCs were calibrated with Poly(2-vinyl pyridines) that were used as standard samples.

Uv–visible spectroscopy

Percent transmittance (*%T*) was determined for the aqueous solutions of $PMPC_{25}$-*b*-$PDMAEMA_n$ (n = 24 and 48) using a JASCO V-630 BIO UV–vis spectrophotometer with a quartz cell path length of 1.0 cm at various temperatures. Here, during the experiment the temperature was changed from 25 to 70 °C with a heating or cooling rate of 1.0 °C/min, and was maintained using a JASCO ETC-717 thermostat system.

Dynamic light scattering (DLS)

DLS was performed using a Zetasizer Nano instrument (Malvern) equipped with a 4 mW He–Ne laser wavelength ($\lambda = 632.8$ nm, scattering angle: 90° and 173°) at 25 °C. Milli-Q water was used to eliminate interference from dust particles. The polymer was dissolved in water and then filtered through 0.2 µm nylon filters to prepare sample solutions. After equilibrating samples for 10 min at each temperature change, all measurements were taken. Different parameters obtained, namely hydrodynamic radius (R_h), and light scattering intensity (LSI) were analyzed using Malvern Zetasizer 7.11 software.

Small-angle neutron scattering (SANS)

The micellar dimension and morphology transition of the investigated DHBCs were evaluated using the neutron scattering experiments carried out at the DHRUVA reactor, BARC, Mumbai, India [38]. Here, 1%w/v solution of DHBCs in presence of [NaCl], M were prepared in D_2O and the samples were measured at 30 °C and 50 °C with different pH. For a good diffusion contrast between the hydrogenated polymers and the solvent phase, D_2O was utilized as a solvent. The copolymer solutions were equilibrated in a 5 mm thick Teflon sealed quartz tube for 24 h. As a monochromator, a beryllium oxide (BeO) filter was used. The neutron beam that was incident had a resolution of 15% and an average wavelength (k) of 5.2. Cross sections for neutron scattering in the range of 0.017 to 0.35 $Å^{-1}$ for scattering vectors have been measured. The obtained data were normalized to absolute cross-sectional units after compensating for background contributions and empty cells. SASFIT software was used to evaluate the SANS data [39, 40].

Computational simulation

The MPC, DMAEMA and MPC-*b*-DMAEMA molecular structures were optimized using density functional theory (DFT) with 3D-molecular electrostatic potential (3D-MEP) at the 3-21G level the Gauss 09W calculation window and the Gauss View 5.0.9 software package. Initially, structures were constructed via choosing one molecule each for MPC, DMAEMA and MPC-*b*-PDMAEMA (1:1) blocks. Molecular geometry and dispersion of electrons expressed in terms of the energy related with the highest occupied molecular orbital (E_{HOMO}) and the lowest unoccupied molecular orbital (E_{LUMO}). Also, the energy gap ($\Delta E = E_{LUMO} — E_{HOMO}$), dipole moment (µ), and total energy (T.E) were computed.

Synthesis

PMPC25 and $PMPC_{25}$-*b*-$PDMAEMA_n$ (*n* = 24 and 48)

In water, MPC (10.0 g, 33.9 mmol), V-501 (152 mg, 0.54 mmol), and CPD (380 mg, 1.36 mmol) were dissolved (33.9 mL). The aqueous solution was degassed by purging argon gas for 30 min. After deoxygenation, the lid was closed and the tube was heated in an oil bath at 70 °C for 2 h. The reaction mixture was dialyzed with pure water for 2 days. To correlate the polymerization time and monomer conversion, ^{1}H-NMR spectroscopy was used. About 98.3% (Table 1) monomer conversion was observed. The freeze-drying technique was used to recover the polymer ($PMPC_{25}$) (9.05 g, 87.2%) (Scheme 2). The number-average molecular weight (M_n(NMR)), DP, and molecular weight distribution (M_w/M_n) were derived from GPC as 7.40×10^3 g/mol, 25, and 1.10, respectively.

$PMPC_{25}$-*b*-$PDMAEMA_n$ ($n = 24$ and 48) were prepared via RAFT controlled radical polymerization (Scheme 2). Initially, the MPC was polymerized via RAFT to obtain the $PMPC_{25}$ macro chain transfer agent (CTA). DMAEMA was then polymerized via $PMPC_{25}$ macro-CTA to prepare $PMPC_{25}$-*b*-$PDMAEMA_n$. For the preparation of $PMPC_{25}$-*b*-$PDMAEMA_{48}$, a pre-determined amount of DMAEMA (1.68 mL, 1.57 g, 10.0 mmol) was neutralized with 6 M HCl in 10.0 mL of water. This mixture was treated with $PMPC_{25}$ (1.48 g, 0.200 mmol, M_n(NMR) = 7.40×10^3 g/mol, $M_w/M_n = 1.10$) and V-501 (22.4 mg, 0.08 mmol) added. Using Ar gas to purge the solution for 30 min, it was deoxygenated for 16 h to carry out the block copolymerization at 70 °C. Using ^{1}H-NMR, the percentage after the reaction was calculated to be 99.7%. The zwitterionic diblock copolymer

Table 1 Number-average degree polymerization (DP), number-average molecular weight (M_n), and molecular weight distribution (M_w/M_n) of $PMPC_{25}$ and $PMPC_{25}$-*b*-$PDMAEMA_n$ ($n = 24$ and 48)

System	Conversion (%) (NMR)	Freeze-drying purity (%)	DP (theo)	M_n (theo)	DP (NMR)	M_n (NMR) ($\times 10^4$) $gmol^{-1}$	M_n (GPC) ($\times 10^4$) $gmol^{-1}$	M_w/M_n
$PMPC_{25}$	98.3	87.2	25	7400	25	7400	14,000	1.10
$PMPC_{25}$-*b*-$PDMAEMA_{24}$	98.6	94.3	25	11,330	24[a]	11,170	17,280	1.11
$PMPC_{25}$-*b*-$PDMAEMA_{48}$	99.7	98.0	50	15,260	48[a]	15,000	20,400	1.12

[a]DP of PDMAEMA block

($PMPC_{25}$-*b*-$PDMAEMA_{48}$) was purified by dialysis against pure water for 1 day. $PMPC_{25}$-*b*-$PDMAEMA_{48}$ was recovered by lyophilization (2.99 g, 98.0%, M_n(NMR) = 1.53×10^4 g/mol, $M_w/M_n = 1.12$). $PMPC_{25}$-*b*-$PDMAEMA_{24}$ was prepared by a procedure similar to that described above (4.27 g, 94.3%, M_n(NMR) = 1.12×10^4 g/mol, $M_w/M_n = 1.11$). The details of DP, M_n, and M_w/M_n data for the synthesized polymers are summarized in Table 1.

Results and discussion

Spectral validation

In order to confirm the chemical structures and estimate the DP and composition of $PMPC_{25}$ and $PMPC_{25}$-*b*-$PDMAEMA_n$ ($n = 24$ and 48) in D_2O, ^{1}H-NMR spectra were recorded (Fig. 1).

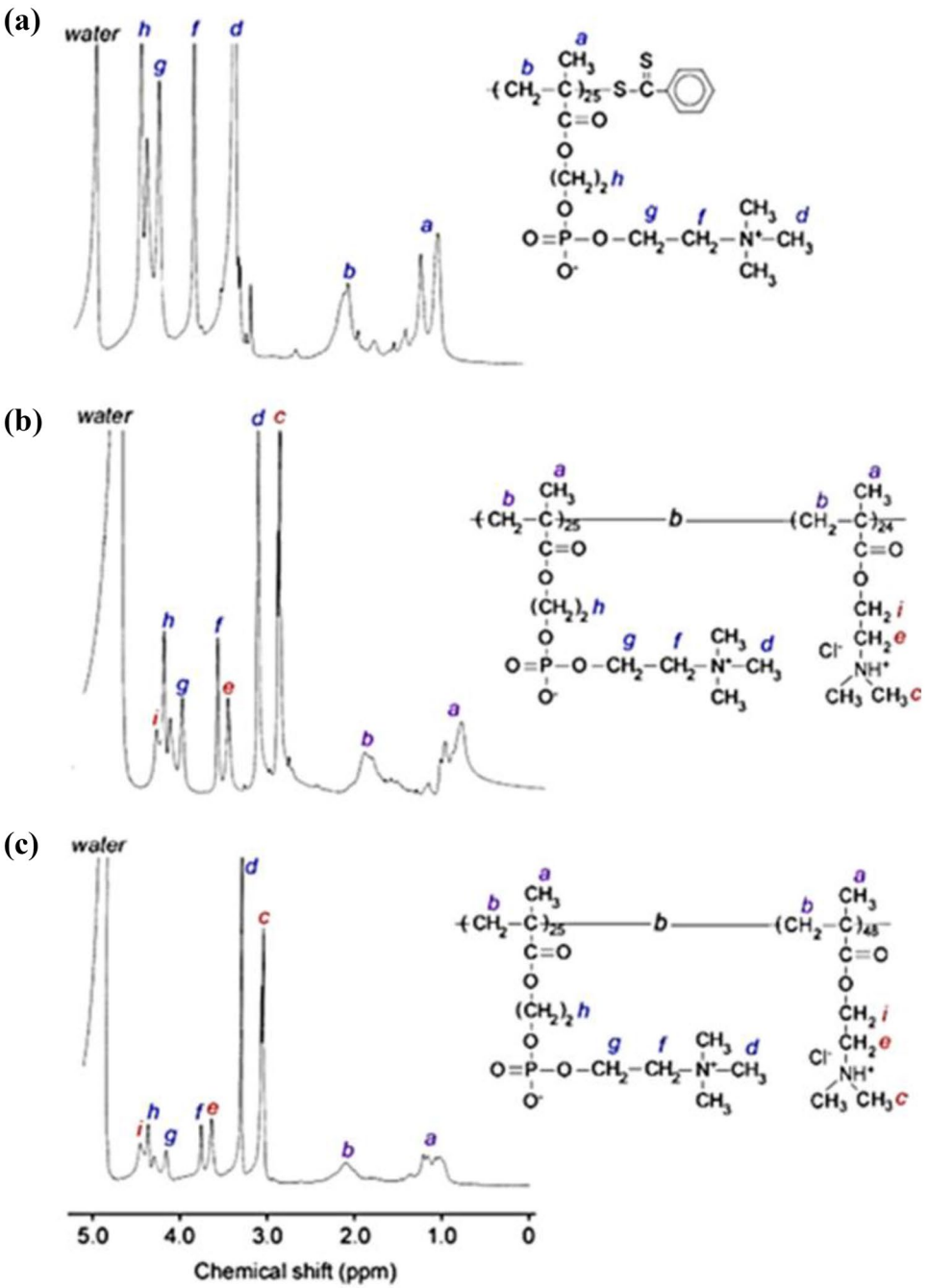

Fig. 1 ^{1}H-NMR spectra of (**a**) $PMPC_{25}$, (**b**) $PMPC_{25}$-*b*-$PDMAEMA_{24}$ and (**c**) $PMPC_{25}$-*b*-$PDMAEMA_{48}$ in D_2O at room temperature

Here, the DP (NMR) value for $PMPC_{25}$ was calculated using the integral intensity ratio of the pendant methylene protons depicted at 3.6 ppm and the terminal phenyl protons at approximately 7.5 ppm. To determine the composition of $PMPC_{25}$-*b*-$PDMAEMA_n$ and its M_n(NMR), the pendant methylene protons in the PMPC block had an integral intensity ratio of 3.2 ppm, while the pendant methyl protons in the PDMAEMA block had an integral intensity ratio of 3.0 ppm. The calculated M_n(theo) values from Eq. (1) agreed with the M_n(NMR) values (Table 1). According to ^{1}H-NMR estimates, the DP(NMR) values for the PDMAEMA blocks present in $PMPC_{25}$-*b*-$PDMAEMA_n$ were 24 and 48, respectively.

The theoretical number-average molecular weight, denoted by the symbol was calculated using the following equation:

$$M_n(\text{theo}) = \frac{[M]_0}{[CTA]_0} \times \frac{P}{100} \times M_m + M_{CTA} \quad (1)$$

where, $[M]_0$ is the initial monomer concentration, $[CTA]_0$ is the initial CTA concentration, p is the percent conversion estimated from ^{1}H-NMR following polymerization, M_m is the molecular weight of the monomer, and M_{CTA} is the molecular weight of CTA.

In agreement with M_n (NMR) ($=7.40\times10^3$ g/mol) calculated from ^{1}H-NMR, M_n(theo) for $PMPC_{25}$ was 7.40×10^3 g/mol. *Mw/Mn* for $PMPC_{25}$ was 1.10, which was low (Fig. 1). These results suggest that a controlled mechanism was used to carry out the RAFT polymerization of MPC. Therefore, $PMPC_{25}$ has a terminal dithiobenzoate group that can be used as a *macro-CTA* to prepare block copolymers.

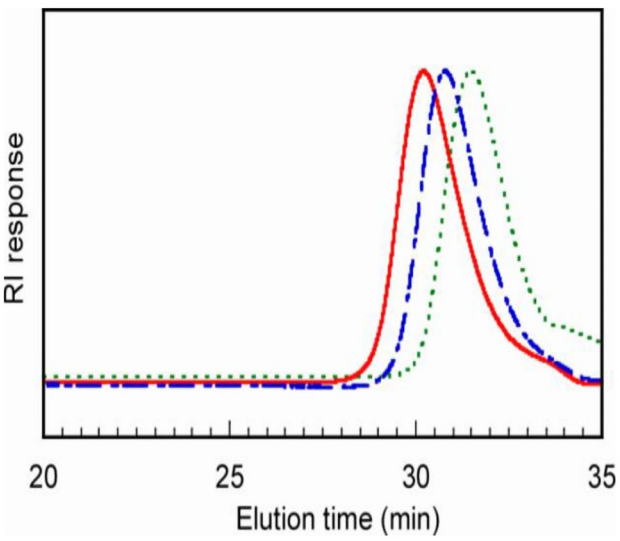

Fig. 2 GPC elution curves of $PMPC_{25}$ (···), $PMPC_{25}$-*b*-$PDMAEMA_{24}$ (- — -), and $PMPC_{25}$-*b*-$PDMAEMA_{48}$ (—) at 40 °C using 0.3 M sodium sulfate aqueous solution having 0.5 M acetic acid

Fig. 3 Structural optimization of (**a**) MPC, (**b**) DMAEMA, and (**c**) ▶ MPC-*b*-DMAEMA (1:1) block with 3D-molecular electrostatic potential (3D-MEP) surface counterplots

Chromatography route

By this technique, molecules are separated according to their size and molecular characteristics, such as composition, molecular weight, and structure. This method has proven to be convenient, rapid, and accurate for analyzing copolymers. We estimated M_n(GPC) and M_w/M_n in Fig. 2. The GPC elution curves measured for $PMPC_{25}$ and $PMPC_{25}$-*b*-$PDMAEMA_n$ ($n=24$ and 48) where GPC elution bands are unimodal with a narrow range of M_w/M_n values below 1.10, 1.11, and 1.12 respectively signifying a well-controlled structure of the block copolymer (Table 1).

Computational simulation

A DFT-based computational simulation is made accessible to examine the understanding of the hydrogen-bonding interaction mechanism in $PMPC_{25}$-*b*-$PDMAEMA_n$ ($n=24$ and 48) based zwitterionic block-neutral block copolymer. This may provide further clarity into the stability of the two BCPs from various optimized descriptors evaluated.

Here, the total energy (T.E) reveals the stability of the molecules. The more negative value of T.E, the more is the stability of the block. All the block (MPC, DMAEMA, and MPC-*b*-DMAEMA) show negative energy. The dipole moment (μ), as a metric of molecular interaction is also presented. Like the stated results, μ demonstrated an increase in its values thereby indicating a favorable accumulation of PMPC in PDMAEMA, which enhances effective interaction between the two BCPs. The literature investigations have shown that the favorable interactions are caused by the lower ΔE value and higher E_{HOMO} value [41]. The energy gap (ΔE), which is the distinction between the energy of E_{HOMO} and E_{LUMO}, shows how well PMPC and PDMAEMA blocks interact. The lowest ΔE (−0.1683 eV) and highest E_{HOMO} (−0.0139 eV) values are seen in our case that depicted favorable interaction in the examined DHBC. In addition, the 3D-molecular electrostatic potential (3D-MEP) or color spectrum is provided to offer a visual insight explaining the intermolecular interaction/nucleation between MPC, DMAEMA, and MPC-*b*-DMAEMA polymer model system. Mulliken charge distributions of the atoms were represented in the color spectrum, predicting the electrophilic coordination centers and nucleophilic sites of the polymer block as well as electron charge density distributions. Polymer's nucleophilic regions are indicated by its most negative potential, which is shown in red, while its electrophilic sites are shown in blue (Fig. 3).

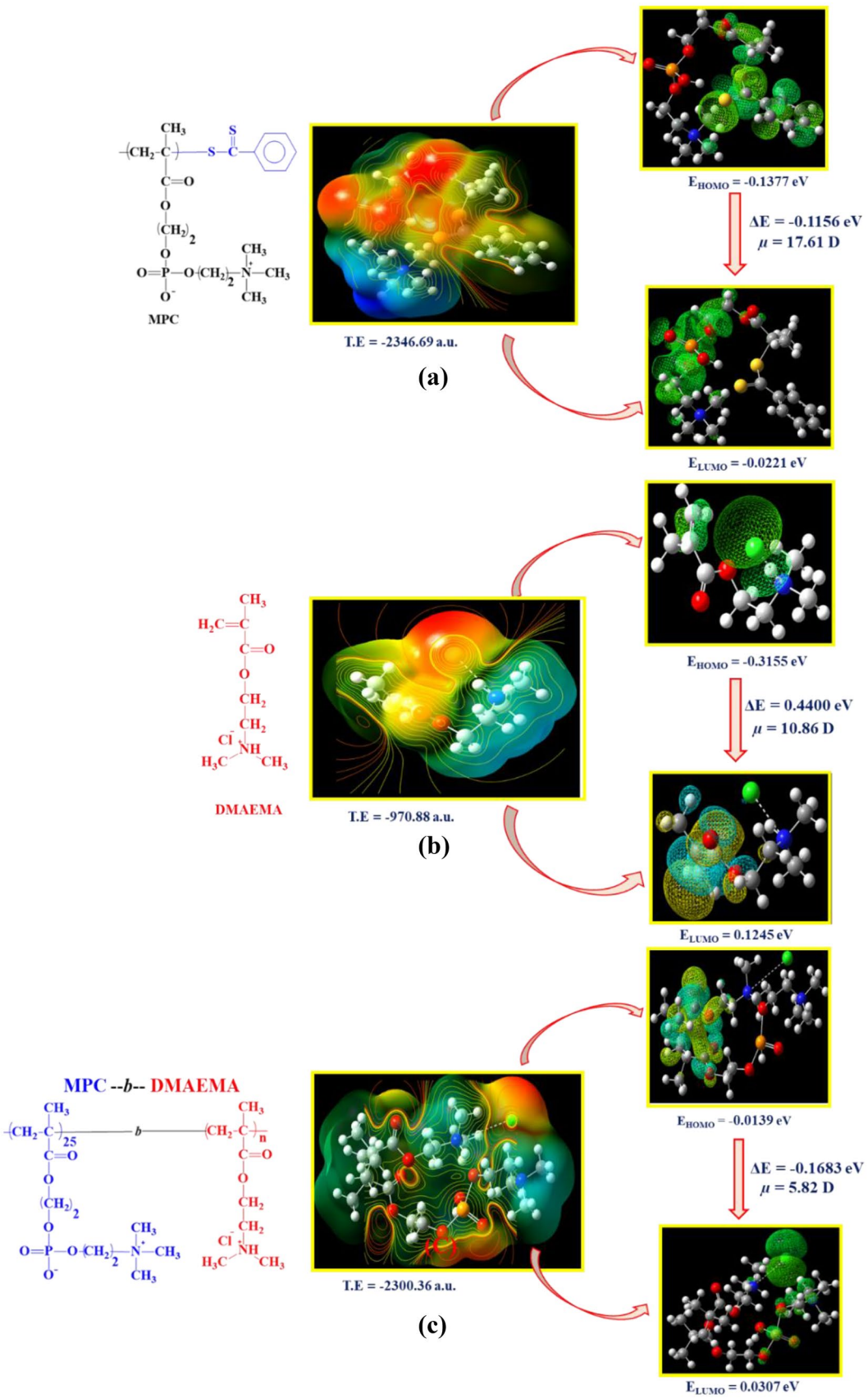
MPC
T.E = -2346.69 a.u.
E_HOMO = -0.1377 eV
ΔE = -0.1156 eV
μ = 17.61 D
E_LUMO = -0.0221 eV
(a)
DMAEMA
T.E = -970.88 a.u.
E_HOMO = -0.3155 eV
ΔE = 0.4400 eV
μ = 10.86 D
E_LUMO = 0.1245 eV
(b)
MPC --b-- DMAEMA
T.E = -2300.36 a.u.
E_HOMO = -0.0139 eV
ΔE = -0.1683 eV
μ = 5.82 D
E_LUMO = 0.0307 eV
(c)

Influence of pH

(i) Spectral analysis

Figure 4 presents the ^{1}H-NMR spectra for PMPC$_{25}$-*b*-PDMAEMA$_n$ ($n = 24$ and 48) recorded in D_2O at pH 3 and 9 to understand the influence of the stimuli (pH) applied.

In acidic environment (pH 3), the protonation occurs at the PDMAEMA block showing the + Inductive effect of that group due to deshielding, resulting in an increase in δ ppm while applying a basic environment (pH 9), the deprotonation occurs at the PDMAEMA block as a result of the -Inductive effect of that group due to shielding effect, which results in a decrease in δ ppm.

For PMPC$_{25}$-*b*-PDMAEMA$_n$ ($n = 24$ and 48) for methylene proton (*e*) in acidic media because of the deshielding effect of the group, the peak appears at 2.3 ppm. While in basic media because of the shielding effect of the group, the peak shifts to 2.7 ppm. In the case of pedant methyl proton (*c*), intensity varies due to shielding and deshielding effects. Here, we conclude that in the case of a small number of monomers or DP ($n = 24$) with less hydrophobic interaction, there will be no change in acidic or basic media, while with high DP ($n = 48$), due to the deprotonation of the PDMAEMA block with enhanced hydrophobic interactions, micellar formation is expected forming the micellar core.

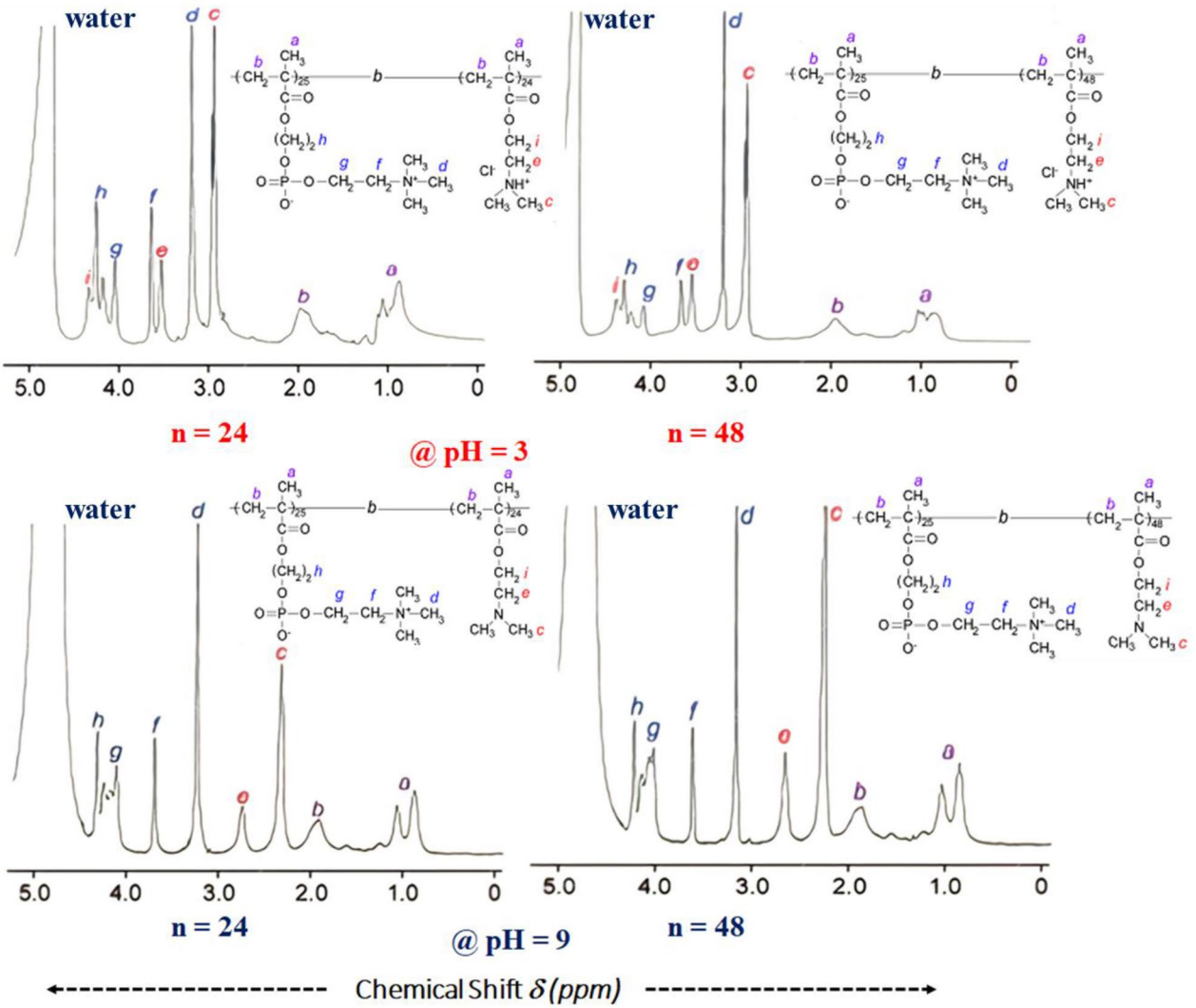

Fig. 4 ^{1}H-NMR spectra of PMPC$_{25}$-*b*-PDMAEMA$_n$ ($n = 24$ and 48) at different pH in D_2O at room temperature. The labels (**a**–**g**) marked in the spectra are referred in Fig. 1

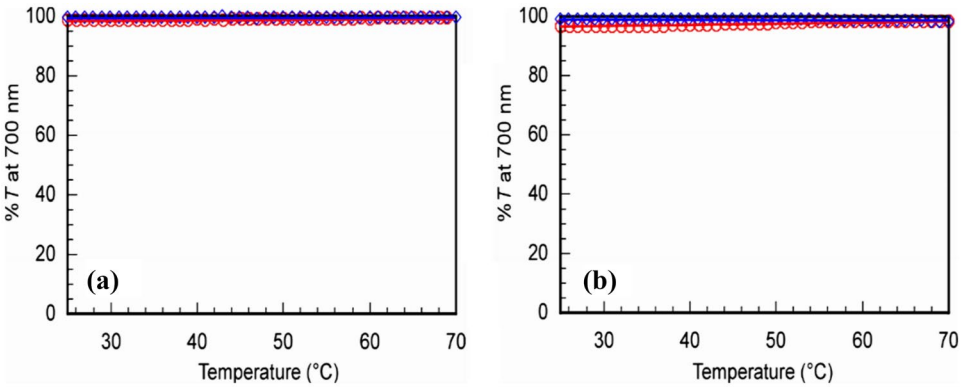

Fig. 5 Temperature dependence of the percent transmittance (%*T*) at 700 nm for (**a**) $PMPC_{25}$-*b*-$PDMAEMA_{24}$ (**b**) $PMPC_{25}$-*b*-$PDMAEMA_{48}$ in 0.1 M NaCl (1%w/v) at pH 12 with heating (○) and cooling (◇)

(ii) Turbidimetry

The temperature dependence of percent transmittance (%*T*) or turbidity measurements of aqueous solutions for $PMPC_{25}$-*b*-$PDMAEMA_{24}$ and $PMPC_{25}$-*b*-$PDMAEMA_{48}$ in 0.1 M NaCl (1%w/v) at pH 12 were performed to determine the LCST behavior of this DHBCs. The graphs of these DHBCs (%*T* versus temperature) are shown in Fig. 5.

The BCP solutions have a basic pH of about 12 when they are dissolved in water at ambient temperature. The solutions are monitored at 700 nm for %*T* measurements. Here, we observed no prominent behavior for both the copolymers at 12 pH values in 0.1 M NaCl, which may be due to weak hydrophobic interaction of the DMAEMA block.

(iii) Scattering conduct

DLS measurements were calculated to acquire a better understanding of the micellar structure of 1%w/v $PMPC_{25}$-*b*-$PDMAEMA_n$ ($n = 24$ and 48) in a 0.1 M NaCl solution and at pH = 12. The R_h values of the DHBCs are determined as a function of temperature as shown in Fig. 6.

For $PMPC_{25}$-*b*-$PDMAEMA_{24}$ at pH 12, it was observed that neither R_h nor LSI increased with increasing temperature. The R_h value of this DHBC depicted its unimer form throughout the temperature variations. Such polymer chains cannot aggregate at high temperatures because the DP of the PDMAEMA block is too small for this block (Fig. 6a).

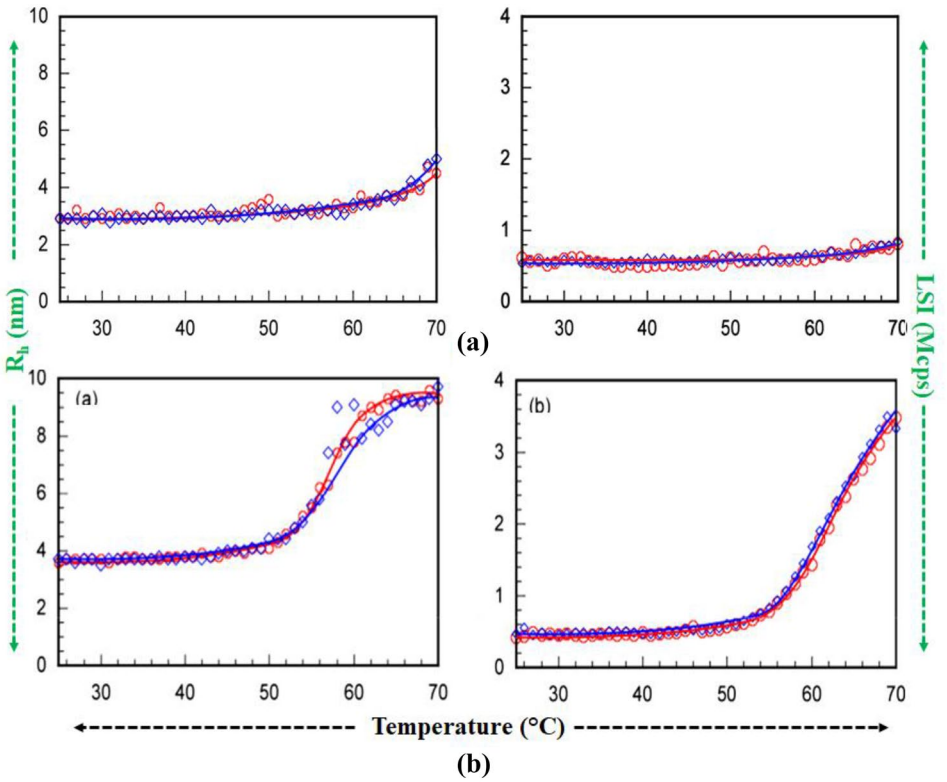

Fig. 6 Temperature dependence R_h and LSI for (**a**) $PMPC_{25}$-*b*-$PDMAEMA_{24}$ and (**b**) $PMPC_{25}$-*b*-$PDMAEMA_{48}$ at pH 12 in 0.1 M NaCl with heating (○) and cooling (◇)

For the $PMPC_{25}$-*b*-$PDMAEMA_{48}$ at pH 12, where both R_h and LSI values continue to increase, a very interesting steep rise in R_h is observed at about 57 °C which inferred the aggregation of the PDMAEMA block thereby associating to form the core of micelles which is consistent with the DHBC ability to form polymer micelles [42–44]. Micelles are produced due to deprotonation of the PDMAEMA block in 0.1 M NaCl environment at varied temperature and also due to the enhanced hydrophobic interaction which can be seen in Fig. 6b.

In addition, DLS was utilized to examine the particle size distribution and temperature-dependent aggregation behavior of $PMPC_{25}$-*b*-$PDMAEMA_n$ ($n = 24$ and 48) in varying NaCl concentrations at both pH levels (Fig. 7).

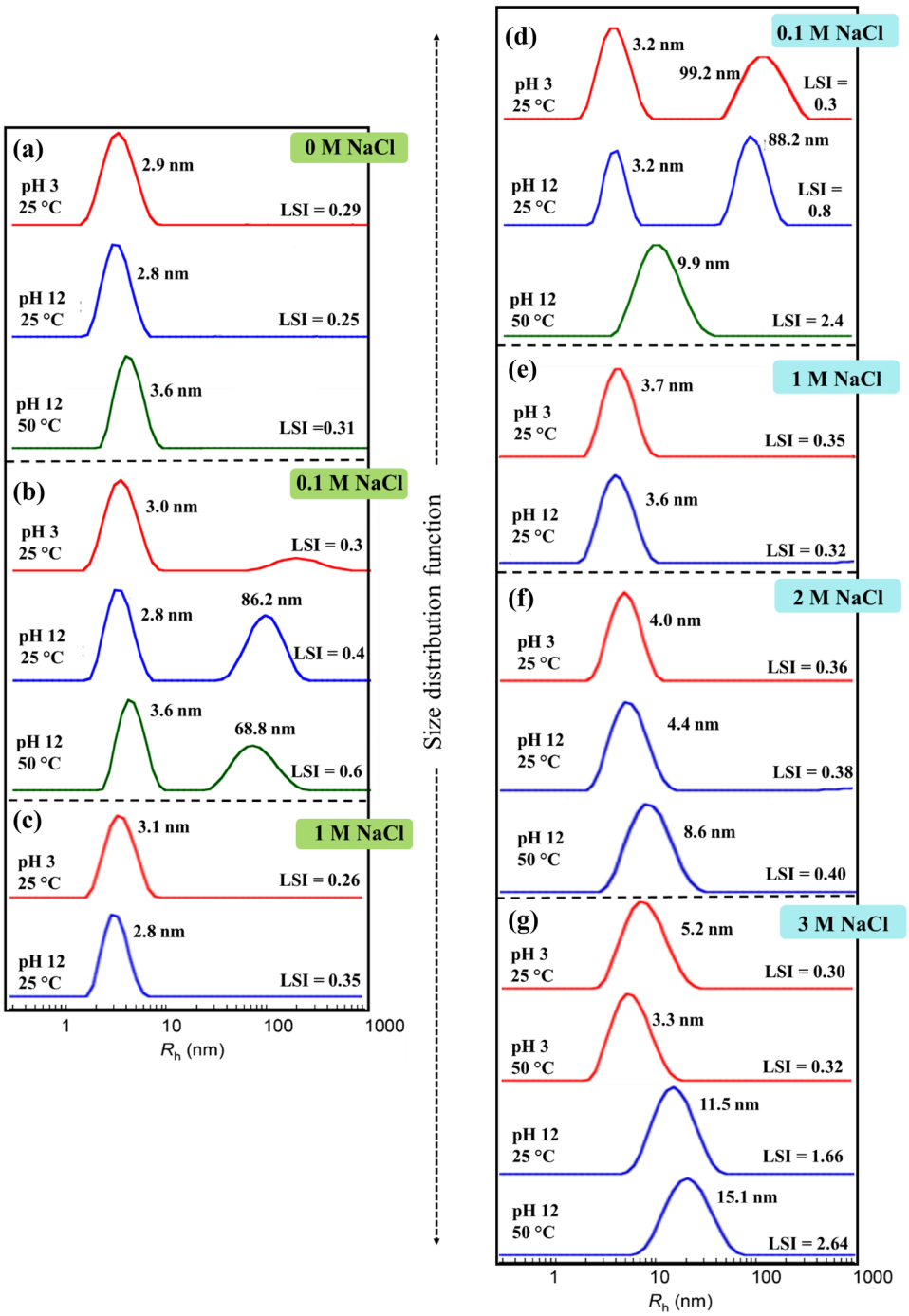

Fig. 7 Hydrodynamic radius (R_h) distributions profile for (1%w/v) $PMPC_{25}$-*b*-$PDMAEMA_n$ with (**a**–**c**) $n = 24$ (d-g) $n = 48$ as a function [NaCl], M at different pH and temperature

Table 2 SANS data of 1%w/v $PMPC_{25}$-*b*-$PDMAEMA_n$ ($n = 24$ and 48) with increasing NaCl concentration and in varying stimuli environments

[NaCl], M	pH	T, (°C)	Micellar parameters		Micellar structure
1%w/v $PMPC_{25}$-b-$PDMAEMA_{24}$					
1.0	3	25	$R_g = 19.6$ Å		Unimers
	12		$R_g = 21.7$ Å		Unimers
1%w/v $PMPC_{25}$-b-$PDMAEMA_{48}$					
1.0	3	25	$R_g = 21.5$ Å		Unimers
	12		$R_g = 22.6$ Å		Unimers
2.0	3	25	$R_g = 22.4$ Å		Unimers
	12	25	$R_g = 23.2$ Å		Unimers
		50	$R_g = 66.0$ Å		Spherical
3.0	3	25	$R_g = 32.5$ Å		Unimers
		50	$R_g = 36.7$ Å		Unimers
	12	25	$R_a = 92.9$ Å,	$R_b = 40.0$ Å	Ellipsoidal
		50	$R_a = 86.1$ Å,	$R_b = 50.4$ Å	Ellipsoidal

R_a and R_b = radius of semi-major and semi-minor axes, R_g = radius of gyration

The particle size distribution of $PMPC_{25}$-*b*-$PDMAEMA_{24}$ in 0.1 M NaCl was unimodal with $R_h = 3.0$ nm and LSI = 0.3 Mcps at pH 3 at 25 °C as shown in Fig. 7b. Bimodal distribution profile was observed at pH 12 at 25 °C, with $R_h = 2.8$ nm, and 86.2 nm, and LSI = 0.4 Mcps part of the PDMAEMA block aggregated due to hydrophobic interactions [45]. Therefore, the temperature was elevated to 50 °C, and DLS was measured at pH 12. As a result, we get a yield of $R_h = 3.6$ and 68.8 nm LSI = 0.6 Mcps is obtained. Furthermore, with increase in the NaCl concentration, i.e., 1.0 M at 25 °C, we found that $PMPC_{25}$-*b*-$PDMAEMA_{24}$ shows unimodal (single peak) size distribution with $R_h = 3.1$ nm and LSI = 0.26 Mcps at pH 3 and $R_h = 2.8$ nm and LSI = 0.35 Mcps at pH 12 respectively (Fig. 7c). However, no changes in R_h distribution and LSI were observed. The PDMAEMA block cannot be aggregated with a high temperature. In the case of $PMPC_{25}$-*b*-$PDMAEMA_{24}$, the polymer chains cannot aggregate at high temperatures, because the DP of the PDMAEMA block is too small. Also, the $PMPC_{25}$-*b*-$PDMAEMA_{24}$ block has relatively low LSI close to 0.6 Mcps, indicating that both copolymers were completely dissolved in water.

The R_h distribution of $PMPC_{25}$-*b*-$PDMAEMA_{48}$ in 0.1 M NaCl is bimodal at pH 3 and 25 °C, with $R_h = 3.2$ and 99.2 nm and LSI = 0.3 Mcps. On the other hand, at pH 12 at 25 °C, we observe $R_h = 3.2$ and 88.2 nm with LSI = 0.8 Mcps. As the temperature is raised to 50 °C, and at pH 12, the R_h distribution becomes unimodal with $R_h = 9.9$ nm, and LSI increase to 2.4 Mcps as shown in Fig. 7d. PDMAEMA has LCST of 40–50 °C. As the temperature rises above its LCST, PDMAEMA's hydrophobic interactions are favored leading to the formation of micelles. The PDMAEMA block was protonated at pH 3 to be in a unimer state. However, the PDMAEMA block was deprotonated at pH 12, which made micelles with the PDMAEMA block core.

Also, the size distribution of $PMPC_{25}$-*b*-$PDMAEMA_{48}$ with increase in the NaCl concentration of 1.0 M, 2.0 M, and 3.0 M NaCl in aqueous solutions at 25 °C was measured using DLS (Fig. 7e–g). We also found that the R_h distributions of $PMPC_{25}$-*b*-$PDMAEMA_{48}$ at pH 3 and 12 were unimodal in the presence of 1.0 M and 2.0 M NaCl solutions (Fig. 7e–f). The PDMAEMA block was protonated at pH 3 to be in a unimer state, respectively. On the other hand, the PDMAEMA block was deprotonated at pH 12, thus forming micelles with the PDMAEMA block core in a 3.0 M NaCl solution (Fig. 7g). Therefore, at pH 12 in a 3.0 M NaCl aqueous solution concentration at 25 °C, the R_h and LSI increased to 11.5 nm and 1.66 Mcps, and with further rising temperature 50 °C the R_h and LSI increased to 15.1 nm and 2.64 Mcps, respectively (Table 2). The PDMAEMA block may aggregate due to the salting-out effect in the presence of 3.0 M NaCl. To comprehend the influence of temperature on the structure of micelle $PMPC_{25}$-*b*-$PDMAEMA_{48}$, we executed SANS measurements of 1%w/v $PMPC_{25}$-*b*-$PDMAEMA_{48}$ solution at pH 3–12 with adding of 3.0 M NaCl at 25 °C and 50 °C, data are shown in Table 2.

The analysis of the neutron scattering properties of 1%w/v $PMPC_{25}$-*b*-$PDMAEMA_n$ ($n = 24$ and 48) at various temperatures and pH in the presence of NaCl salt is depicted in Fig. 8. The absolute scattering intensity patterns are shown in Fig. 8a for 1%w/v $PMPC_{25}$-*b*-$PDMAEMA_{24}$ in varying NaCl solution environments at different pH and temperature. Here, the solid line represents the best fit to the resulting radius, also known as the radius of gyration (R_g) which is found to be 19.6 Å and 21.7 Å that gives a clear indication of the presence of Gaussian chain distribution or unimers (Table 2).

A similar profile was observed for 1%w/v $PMPC_{25}$-*b*-$PDMAEMA_{48}$ in the presence of varying NaCl concentration as shown in Fig. 8b. For the 2.0 M NaCl solution at 25 °C and 12 pH, the examined BCP showed R_g values as 23.2 Å which is a clear indicator of unimers. Furthermore, a noticeable change was observed which depicted spherical micelle with R_g as 66.0 Å in the same NaCl concentration at pH 12 and at 50 °C (Table 2). As predicted, the R_g value of $PMPC_{25}$-*b*-$PDMAEMA_{48}$ is greater than $PMPC_{25}$-*b*-$PDMAEMA_{24}$ which is due to the longer PDMAEMA block in $PMPC_{25}$-*b*-$PDMAEMA_{48}$.

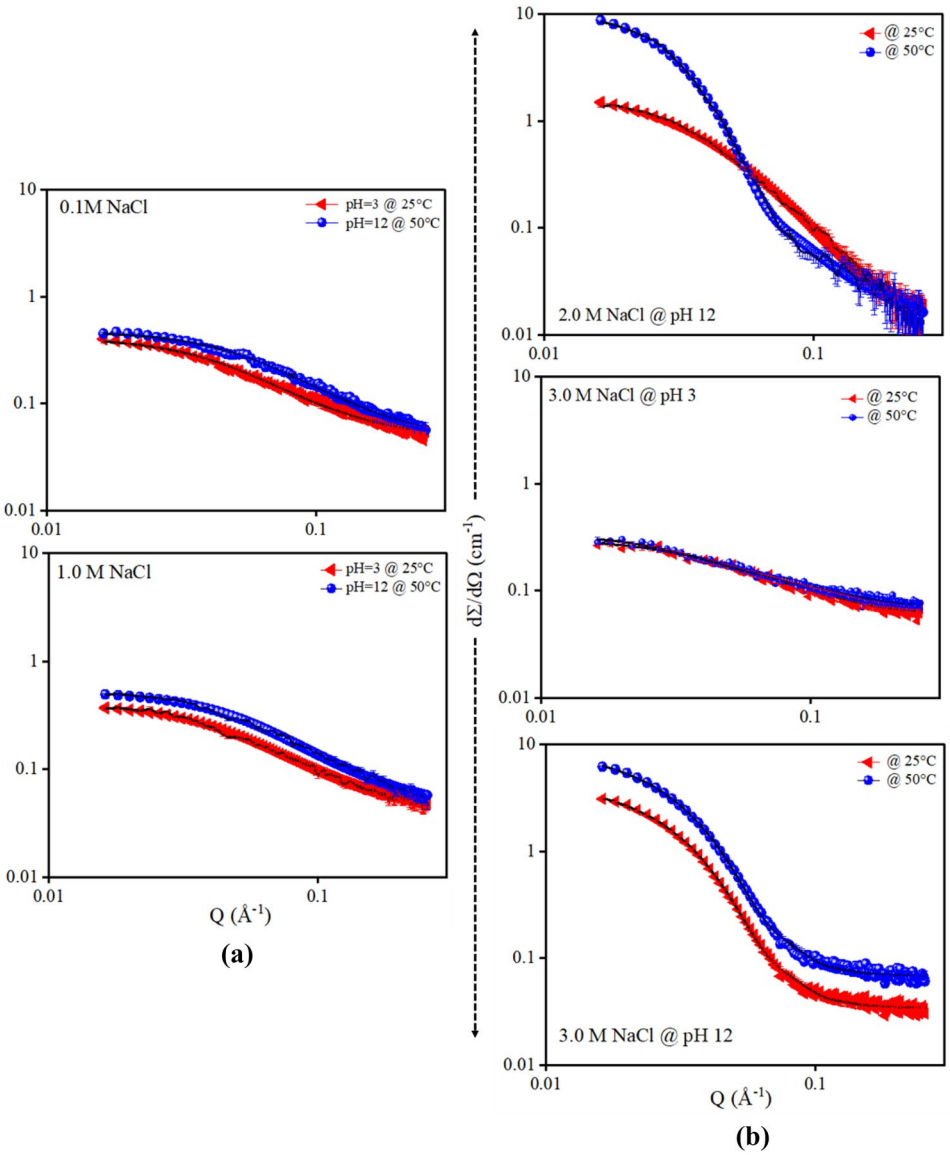

Fig. 8 Normalized scattering cross-section pattern (dΣ/dΩ) as a function of the scattering vector Q for (**a**) 1%w/v $PMPC_{25}$-*b*-$PDMAMEA_{24}$ and (**b**) 1%w/v $PMPC_{25}$-*b*-$PDMAMEA_{48}$ in varying NaCl solution environment at different pH and temperature

The scattering intensity of 1%w/v $PMPC_{25}$-*b*-$PDMAEMA_{48}$ at 3 pH is practically unchanged, i.e., it remains Gaussian chain (unimers) in the presence of 3.0 M NaCl at 25 °C and 50 °C. The electrostatic repulsions were screened by adding NaCl to the solution which generated the aggregates with R_g of 32.5 Å and 36.7 Å similar to systems where salt is absent, and dissolved as unimers (Table 2). However, in pH 12, the scattering intensity increases with a noticeable shift and Q dependency shows block copolymer aggregation into core–shell spherical, ellipsoidal micelles which are schematically depicted in Scheme 3. Here, the ellipsoidal micelles model is assumed to suit the results, and hence the data are fitted accordingly.

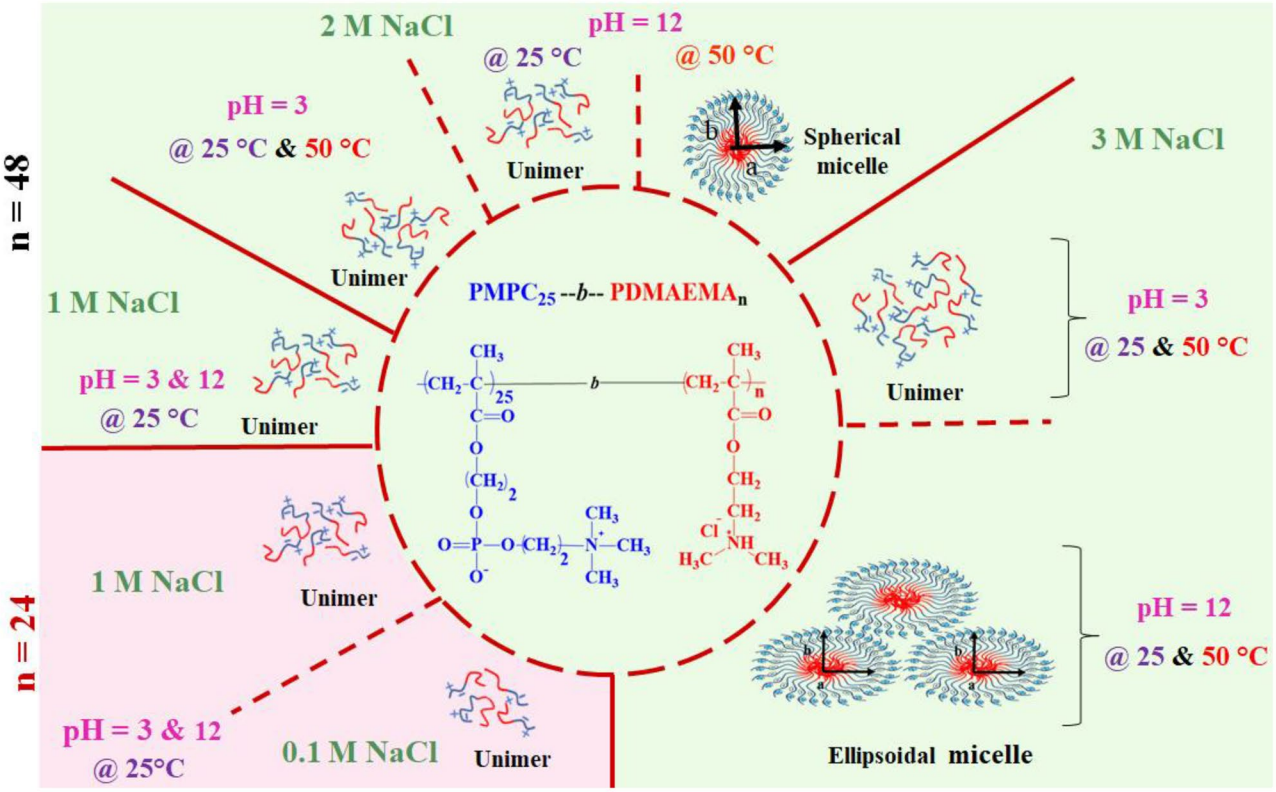

Scheme 3 Display of varied self-assembly generation in aqueous solution of stimuli (pH andtemperature) responsive $PMPC_{25}$-*b*-$PDMAEMA_n$ ($n = 24$ and 48)

Conclusion

This research develops a connection between the computational strategy and the experimental findings. This study reports successful synthesis of DHBCs $PMPC_{25}$-*b*-$PDMAEMA_n$ ($n = 24$ and 48) with low polydispersity index (~ 1.0), controlled molecular weight, and a well-controlled structure (1.10–1.12 M_w/M_n) using RAFT polymerization. The intermolecular interactions as depicted from ΔE (− 0.1683 eV) and E_{HOMO} (− 0.0139 eV) values showed favorable interactions, which perfectly correlate with the experimental findings. Further, the spectral and chromatographic study affirmed the correct formation of these DHBCs. Scattering estimates inferred the ability of DHBCs to form nanoscale core–shell aggregates in aqueous solution as a function of applied stimuli (temperature and pH). It was found that both polymers generally behave as unimers in aqueous solution at low temperature and as the temperature increases, they form large core–shell aggregates, i.e., $PMPC_{25}$-*b*-$PDMAEMA_{48}$ forms spherical and ellipsoidal micelles where PDMAEMA forms core and PMPC block surrounding it. Thus, the obtained results in this study indicate the potential utility of the newly synthesized DHBCs as useful nanocarriers for therapeutic applications.

Acknowledgements The authors acknowledge the scientists Dr. Vinod K. Aswal and Dr. Debes Ray, Solid State Physics Division, Bhabha Atomic Research Centre (BARC), Mumbai, Maharashtra-India for providing the neutron scattering facility and also to the Department of Chemistry, Sardar Vallabhbhai National Institute of Technology (SVNIT), Surat, Gujarat-INDIA for providing the central instrumentation facility.

Declarations

Ethics approval No human or animal subjects were used in this research.

Competing interests The authors declare no competing interests.

References

1. Varvara C, Stergios P (2018) Stimuli-responsive amphiphilic PDMAEMA-*b*-PLMA copolymers and their cationic and zwitterionic analogs. Polym Sci A Polym Chem 56(6):598–610. https://doi.org/10.1002/pola.28931
2. Cyrille B, Nathaniel Alan C, Kenward J, Diep N, Thuy-Khanh N, Nik NM, A, Susan O, Sivaprakash S, Jonathan Y (2016) Copper-mediated living radical polymerization (atom transfer radical polymerization and copper (0) mediated polymerization): from fundamentals to bioapplications. Chem Rev 116(4):1803–1949. https://doi.org/10.1021/acs.chemrev.5b00396

3. Aguilar R, Elvira C, Gallardo A, Vazquez B, Román J (2007) Smart polymers and their applications as biomaterials, Biomaterials. SPAIN 3(6) 1–27 chapter-6. https://www.researchgate.net/publication/228365910
4. Eun Seok G, Samuel MH (2004) Stimuli-reponsive polymers and their bioconjugates Prog Polym Sci 29(12)1173–1222
5. Vitaliy VK, Theoni KG (2018) Temperature-responsive polymers: chemistry, properties, and applications, John Wiley & Sons, U.K. https://doi.org/10.1002/9781119157830
6. Stephanie G, Mohamed E, El-Sayed H (2010) Stimuli-sensitive particles for drug delivery. Nat Rev Drug Discov 171–190 chapter-7. https://doi.org/10.1142/97898142956800008
7. Jiao B, Mingzu Z, Jinlin H, Peihong N (2013) Preparation and self-assembly of double hydrophilic poly (ethylethylene phosphate)-block-poly [2-(succinyloxy) ethyl methacrylate] diblock copolymers for drug delivery. React Funct Polym 73(3):579–587. https://doi.org/10.1016/j.reactfunctpolym.2012.12.010
8. Ren J (2011) Biodegradable poly (lactic acid): synthesis, modification, processing and applications Springer Science and Business Media New York 978-3-642-17595-4
9. Khimani M, Yusa S, Nagae A, Enomoto R, Aswal V, Kesselman E, DaninoD BP (2015) Self-assembly of multi-responsive poly (N-isopropylacrylamide)-*b*-poly (N, N-dimethylaminopropylacrylamide) in aqueous media. Springer Science and Business Media 69:96–109. https://doi.org/10.1016/j.eurpolymj.2015.05.027
10. Agut W, Brûlet A, Schatz C, Taton D, Lecommandoux S (2010) pH and temperature responsive polymeric micelles and polymersomes by self-assembly of poly [2-(dimethylamino) ethyl methacrylate]-*b*-poly (glutamic acid) double hydrophilic block copolymers. Langmuir 26(13):10546–10554. https://doi.org/10.1021/la1005693
11. Kumar S, Parikh K (2012) Influence of temperature and salt on association and thermodynamic parameters of micellization of a cationic gemini surfactant. J Appl Sol 1(1):65–73. E-ISSN:1929–5030/12
12. Kumar S, Sharma D, Kabir-ud-Din (2003) Temperature-[salt] compensation for clouding in ionic micellar systems containing sodium dodecyl sulfate and symmetrical quaternary bromides. Langmuir 19(8):3539–3541. https://doi.org/10.1021/la026783e
13. Zhang Z, Moxey M, Alswieleh A, Morse J, Lewis L, Geoghegan M, Leggett J (2016) Effect of salt on phosphorylcholine-based zwitterionic polymer brushes. Langmuir 32(20):5048–5057. https://doi.org/10.1021/acs.langmuir.6b00763
14. Saha P, Palanisamy R, Santi M, Ganguly R, Mondal S, Singha K, Pich A (2021) Thermoresponsive zwitterionic poly (phosphobetaine) microgels: effect of macro-RAFT chain length and cross-linker molecular weight on their antifouling properties. Polym Adv Technol 32(7):2710–2726. https://doi.org/10.1002/pat.5214
15. Goda T, Ishihara K, Miyahara Y (2015) Critical update on 2-methacryloyloxyethyl phosphorylcholine (MPC) polymer science. J Appl Polym Sci 132(16). https://doi.org/10.1002/app.41766
16. Hong L, Zhang Z, Zhang Y, Zhang W (2014) Synthesis and self-assembly of stimuli-responsive amphiphilic block copolymers based on polyhedral oligomeric silsesquioxane. J Polym Sci A Polym Chem 52(18):2669–2683. https://doi.org/10.1002/pola.27287
17. Lewis A, Tang Y, Brocchini S, Choi W, Godwin A (2008) Poly (2-methacryloyloxyethyl phosphorylcholine) for protein conjugation. Bioconjugate Chem 19(11):2144–2155. https://doi.org/10.1021/bc800242t
18. Kuroda K, Miyoshi H, Fujii S, Hirai T, Takahara A, Nakao A, Iwasaki Y, Morigaki K, Ishihara K, Yusa SI (2015) Poly (dimethylsiloxane)(PDMS) surface patterning by biocompatible photocrosslinking block copolymers. RSC Adv 5(58):46686–46693. https://doi.org/10.1039/C5RA08843G
19. Bütün V, Armes P, Billingham C (2001) Synthesis and aqueous solution properties of near-monodisperse tertiary amine methacrylate homopolymers and diblock copolymers. Polym J 42(14):5993–6008. https://doi.org/10.1016/S0032-3861(01)00066-0
20. Atanase LI, Desbrieres J, Riess G (2017) Micellization of synthetic and polysaccharides-based graft copolymers in aqueous media. Prog Polym Sci 73:32–60. https://doi.org/10.3390/polym3031065
21. Ma Y, Lobb J, Billingham C, Armes P, Lewis L, Lloyd W, Salvage J (2002) Synthesis of biocompatible polymers. 1. Homopolymerization of 2-methacryloyloxyethyl phosphorylcholine via ATRP in protic solvents: an optimization study. Macromolecules. 35(25):9306–9314. https://doi.org/10.1021/ma0210325
22. Plamper FA, Synatschke CV, Majewski AP, Schmalz A, Schmalz H, Müller AH (2014) Star-shaped poly [2-(dimethylamino) ethyl methacrylate] and its derivatives: toward new properties and applications. Polimery 59(1):66–73. https://doi.org/10.14314/polimery.2014.066
23. Niskanen J, Wu C, Ostrowski M, Fuller G, Hietala S, Tenhu H (2013) Thermoresponsiveness of PDMAEMA. Electrostatic and stereochemical effects, Macromolecules 46(6):2331–2340. https://doi.org/10.1021/ma302648w
24. Mitsukami Y, Donovan S, Lowe B, McCormick L (2001) Water-soluble polymers. 81. Direct synthesis of hydrophilic styrenic-based homopolymers and block copolymers in aqueous solution via RAFT. Macromolecules 34(7):2248–2256. https://doi.org/10.1021/ma0018087
25. Stubbs E, Laskowski E, Conor P, Heinze A, Karis D, Glogowski M (2017) Control of pH-and temperature-responsive behavior of mPEG-*b*-PDMAEMA copolymers through polymer composition. J Macromol Sci A 54(4):228–235. https://doi.org/10.1080/10601325.2017.1282694
26. Han X, Zhang X, Zhu H, Yin Q, Liu H, Hu Y (2013) Effect of composition of PDMAEMA-*b*-PAA block copolymers on their pH-and temperature-responsive behaviors. Langmuir 29(4):1024–1034. https://doi.org/10.1021/la3036874
27. Mohammadi M, Salami-Kalajahi M, Roghani-Mamaqani H, Golshan M (2017) Effect of molecular weight and polymer concentration on the triple temperature/pH/ionic strength-sensitive behavior of poly (2-(dimethylamino) ethyl methacrylate). Int J Polym Mater 66(9):455–461. https://doi.org/10.1080/00914037.2016.1236340
28. Plamper FA, Ruppel M, Schmalz A, Borisov O, Ballauff M, Müller AH (2007) Tuning the thermoresponsive properties of weak polyelectrolytes: aqueous solutions of star-shaped and linear poly (N, N-dimethylaminoethyl methacrylate). Macromolecules 40(23):8361–8366. https://doi.org/10.1021/ma071203b
29. Gohy F, Antoun S, Jérôme R (2001) pH-dependent micellization of poly (2-vinylpyridine)-block-poly((dimethylamino) ethyl methacrylate) diblock copolymers. Macromolecules 34(21):7435–7440. https://doi.org/10.1021/ma010535s
30. Manouras T, Koufakis E, Anastasiadis H, Vamvakaki M (2017) A facile route towards PDMAEMA homopolymer amphiphiles. Soft Matter 13(20):3777–3782. https://doi.org/10.1039/C7SM00365J
31. Zhu J, Tan B, Du X (2008) Preparation and self-assembly behavior of polystyrene-block-poly (dimethylaminoethyl methacrylate) amphiphilic block copolymer using atom transfer radical polymerization. Express Polym Lett 2(3):214–225. https://doi.org/10.3144/expresspolymlett.2008.26
32. de Paz BV, Robinson L, Armes P (2000) Synthesis and solution properties of dimethylsiloxane-2-(dimethylamino) ethyl methacrylate block copolymers. Macromolecules 33(2):451–456. https://doi.org/10.1021/ma991665s
33. Ni H, Pan S, Zha S, Wang C, Elaïssari A, Fu K (2002) Syntheses and characterizations of poly [2-(dimethylamino) ethyl methacrylate]-poly (propylene oxide)-poly [2-(dimethylamino)

ethyl methacrylate] ABA triblock copolymers. J Polym Sci A Polym Chem 40(4):624–631. https://doi.org/10.1002/pola.10144
34. Cabral H, Miyata K, Osada K, Kataoka K (2018) Block copolymer micelles in nanomedicine applications. Chem Rev 118(14):6844–6892. https://doi.org/10.1021/acs.chemrev.8b00199
35. Bhadoria A, Kumar S, Aswal VK, Kumar S (2015) Mechanistic approach on heat induced growth of anionic surfactants: a clouding phenomenon. RSC Adv 5(30):23778–23786. https://doi.org/10.1039/C5RA01090J
36. Zhang C, Maric M (2011) Synthesis of stimuli-responsive, water-soluble poly[2-(dimethylamino)ethyl methacrylate/styrene] Statistical Copolymers by Nitroxide Mediated Polymerization. Polymers 1398–1422. https://doi.org/10.3390/polym3031398
37. Sharma D, Khan ZA, Aswal VK, Kumar S (2006) Clouding phenomenon and SANS studies on tetra-n-butylammonium dodecylsulfate micellar solutions in the absence and presence of salts. J Colloid Interface Sci 302(1):315–321. https://doi.org/10.1016/j.jcis.2006.06.021
38. NguyenL IK, Yusa SI (2022) Separated micelles formation of pH-responsive random and block copolymers containing phosphorylcholine groups. Polymers 14(3):577. https://doi.org/10.3390/polym14030577
39. Giacomelli C, Le Men L, Borsali R, Lai-Kee-Him J, Brisson A, Armes SP, Lewis L (2006) Phosphorylcholine-based pH-responsive diblock copolymer micelles as drug delivery vehicles: light scattering, electron microscopy, and fluorescence experiments. Biomacromol 7(3):817–828. https://doi.org/10.1021/bm0508921
40. Aswal K, Goyal S (2000) Small-angle neutron scattering diffractometer at Dhruva reactor. Curr Sci 79(7):947–953. https://www.jstor.org/stable/24104808
41. Jangir A, Patel D, More R, Parmar A, Kuperkar K (2019) New insight into experimental and computational studies of Choline chloride-based 'green'ternary deep eutectic solvent (TDES). Colloids Surf A Physicochem Eng Asp 1181:295–299. https://doi.org/10.1016/j.molstruc.2018.12.106
42. Fukumoto H, Ishihara K, Yusa SI (2021) Thermo-responsive behavior of mixed aqueous solution of hydrophilic polymer with pendant phosphorylcholine group and poly (acrylic acid). Polymers 13(1):148. https://doi.org/10.3390/polym13010148
43. Ukawa M, Akita H, Masuda T, Hayashi Y, Konno T, Ishihara K, Harashima H (2010) 2-Methacryloyloxyethyl phosphorylcholine polymer (MPC)-coating improves the transfection activity of GALA-modified lipid nanoparticles by assisting the cellular uptake and intracellular dissociation of plasmid DNA in primary hepatocytes. Biomaterials 31(24):6355–6362. https://doi.org/10.1016/j.biomaterials.2010.04.031
44. de Castro E, Ribeiro A, Alavarse C, Albuquerque J, da Silva C, Jäger E, Surman F, Schmidt V, Giacomelli C, Giacomelli C (2018) Nanoparticle–cell interactions: surface chemistry effects on the cellular uptake of biocompatible block copolymer assemblies. Langmuir 34(5):2180–2188. https://doi.org/10.1021/acs.langmuir.7b04040
45. Atanase LI, Riess G (2011) Thermal cloud point fractionation of poly (vinyl alcohol-co-vinyl acetate): partition of nanogels in the fractions. Polymers 3(3):1065–1075. https://doi.org/10.3390/polym3031065